An Anthracene Carboxamide-Based Fluorescent Probe for Rapid and Sensitive Detection of Mitochondrial Hypochlorite in Living Cells

Xueling Liu , Guangshuai Zhou , Yali Wang * , Wenzhou Zhang *

Posted Date: 16 August 2023

doi: 10.20944/preprints202308.1195.v1

Keywords: hypochlorite; mitochondria; anthracene carboxyimide; fluorescent probe

Article

An Anthracene Carboxamide-Based Fluorescent Probe for Rapid and Sensitive Detection of Mitochondrial Hypochlorite in Living Cells

Xueling Liu [1,2], Guangshuai Zhou [2], Yali Wang [2,3,*] and Wenzhou Zhang [1,*]

[1] Department of Pharmacy, The Affiliated Cancer Hospital of Zhengzhou University & Henan Cancer Hospital, Zhengzhou 450008, China
[2] School of Pharmaceutical Science and Technology, Health Sciences Platform, Tianjin University, Tianjin 300072, China
[3] Department of Chemistry, College of Pharmacy, North China University of Science and Technology, Tang Shan, 063000, China
* Correspondence: wangyali1105@tju.edu.cn (Y.W.); zlyyzhangwenzhou0551@zzu.edu.cn (W.Z.)

Abstract: Mitochondrial hypochlorite (ClO^-) plays important and often contradictory roles in maintaining the redox balance of mitochondria. Abnormal ClO^- levels can induce mitochondrial inactivation and further cause cell apoptosis. Herein. we have developed an anthracene carboxyimide-based fluorescent probe **mito-ACS** for imaging mitochondrial ClO^- in living cells. This probe exhibits some distinctive features as excellent resistance to photobleaching, high selectivity and sensitivity, as well as good water solubility. **Mito-ACS** showed a noticeable fluorescence response toward ClO^- with a fast response (within 6 s) and a low detection limit (23 nM). Moreover, the introduction of triphenylphosphonium makes the probe soluble in water and selectively localizes to mitochondria. Furthermore, **mito-ACS** was successfully applied to image mitochondria ClO^- in living cells with low toxicity. Remarkably. the less used fluorophore anthracene carboxyimide exhibiting excellent photostability and desirable optical properties provides a promising application prospect in biological systems.

Keywords: hypochlorite; mitochondria; anthracene carboxyimide; fluorescent probe

1. Introduction

Hypochlorite/hypochlorous acid (ClO^-/HOCl), one of the most important reactive oxygen species (ROS), play vital roles in biological activities and daily life [1–3]. ClO^- is commonly used as a household bleach and a disinfectant [4]. More importantly, ClO^- is linked to diverse physiological and pathological functions, especially in the immune defense system [5–7]. But the abnormal production of ClO^- can also result in tissue damage and remodeling with profound implications for many human diseases such as arthritis, cardiovascular disease, and even cancer [8–11]. The mitochondria, as an "energy factory", are considered the main source of ROS in cells including ClO^- [12,13]. It has been reported that abnormal ClO^- can destroy the mitochondrial permeability transport pores and apoptosis signal molecules, leading to a nonspecific increase in membrane permeability and cell damage [14,15]. Therefore, exploring reliable methods for monitoring ClO^- in mitochondria is still in high demand.

The results of nearly a decade have amply demonstrated the advantages and practical applications of fluorescent probes for the detection of reactive oxygen species [16–18]. Also, with the development of fluorescence detection systems, fluorescence analysis is more likely to become the first choice of commonly used detection. More importantly, the development of organelle-targeted fluorescent probes made the precise monitoring of subcellular microenvironments come true [19–21]. To date, a large number of hypochlorite probes have been reported and applied in the biosystem. Each probe indeed possessed its advantages and drawbacks [22–25]. The following points are relevant to the ability of the probe to detect hypochlorite in living organisms and be used for

Preprints (www.preprints.org) | NOT PEER-REVIEWED | Posted: 16 August 2023 doi:10.20944/preprints202308.1195.v1

biological imaging. A key issue is the sensitivity. Due to the and low concentration in living organisms, the probe must respond rapidly to ClO^- and have a low detection limit [26–28]. Another fact is that the probes with good photostability are preferred in the bioimaging application, which can minimize the impact of photobleaching and extend the optical monitoring [29,30]. However, to our knowledge, there are few probes with both characteristics. Hence, developing probes with substantial photostability, sensitivity, and selectivity for monitoring mitochondrial ClO^- becomes our target.

In this work, a new mitochondria-targeted fluorescent probe mito-ACS was rationally designed through the integration of ClO^- sensing thioether, mitochondria targeting triphenylphosphonium cation, and recently developed fluorophore anthracene carboxamide as shown in **Figure 1**. The construction of mito-ACS is on the following facts: first, 1,2-anthracenecarboximide derivatives, similar but prior to 1,8 naphthalimide in many photoproperties including good photostability, visible absorption and emission with a large Stokes shift, and high quantum yield [31–33]. Also, the absorption and fluorescence spectra of anthracenecarboximide could be easily modulated by varying the electron-donating capability of the substituent at the 6-position. Secondly, many studies, including our previous work, have shown that thioethers have high reaction efficiency and selectivity to hypochlorite [34,35]. The thioether with strong electron-donating ability can quench the emission of mito-ACS through an effective (PET) process [36]. And the probe would recover its strong fluorescence once the PET process is blocked by the ClO^- oxidized product sulfoxide. In addition, the introduction of acetylene can obtain a relatively longer analytical wavelength by extending the conjugated length of the aromatic donor part. Third, triphenylphosphine, as a mitochondrial targeting group, can also increase the water solubility of mito-ACS [21]. Based on the principles, mito-ACS exhibits multiple advantages, such as excellent photostability (more than 80 min), large Stokes shift (~ 100 nm), high sensitivity (detection limit of 23 nM), and fast response (within 6 S) toward ClO^-. Moreover, mito-ACS showed good solubility in water, which enables it to be successfully applied to real-time detection of mitochondria ClO^- in biological imaging.

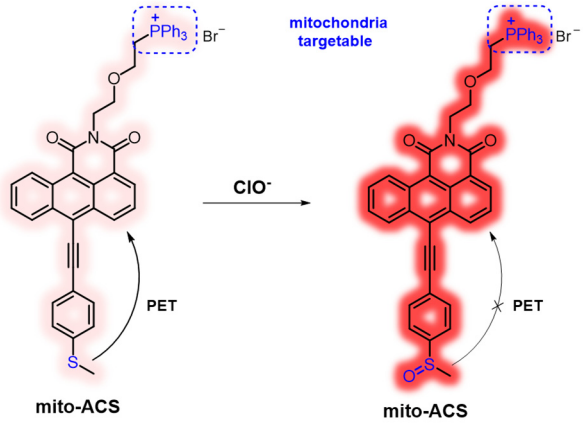

Figure 1. Design Strategy of **mito-ACS** for Sensing ClO^-

2. Materials and Methods

2.1. Reagents and Instruments

Unless otherwise stated, all reagents used for reactions were purchased from commercial suppliers and used without further purification. ^1H NMR and ^{13}C NMR spectra were taken with Bruker Ascend III 400 and Avance III 600 instruments at 298.6 K in $CDCl_3$ and DMSO (d_6). ESI-MS data were acquired on Agilent Technologies 6230 TOF LC/MS with ESI source. UV measurements were carried out on HITACHI U-3900 Spectrophotometer. Fluorescence measurements were carried on Edinburgh FLS980 spectrophotometer, using 450W Xenon lamp. Absolute quantum yields were measured using an integrating sphere detector from Edinburgh Instruments. The ultra-pure water was obtained from Direct-Q5 purifier. HeLa Cells were purchased from Type Culture Collection of

Preprints (www.preprints.org) | NOT PEER-REVIEWED | Posted: 16 August 2023 doi:10.20944/preprints202308.1195.v1

the Chinese Academy of Sciences, Shanghai, China. Fluorescence imaging was studied by a Leica SP 8 confocal laser scanning microscope.

2.2. Synthesis

The anthracene carboxyimide-based probe mito-ACS was synthesized in Scheme 1. Intermediate 1 and 1-Ethynyl-4-(methylthio)benzene were synthesized according to the reported procedures [37,38]. Compund 2 was obtained through Suzuki cross-coupling reaction in 85 % yield, then, it was converted to the bromide adduct 3 through Apple reaction in 82% yield. Finally, the desired product mito-ACS was obtained by treating intermediate 3 with triphenylphosphine in 74% yield. The detailed experimental procedures and characterization data are explained in the Supporting Information.

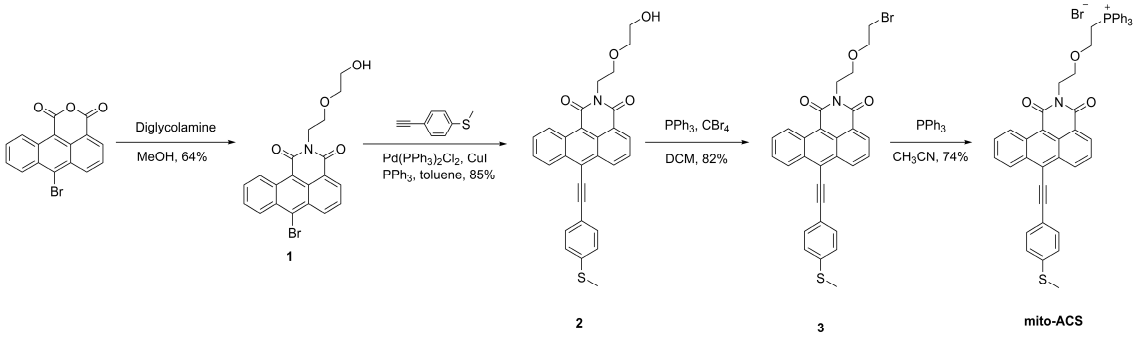

Scheme 1. Synthetic route of **mito-ACS.**

2.3. Preparation of the Spectral Measurements

A stock solution of 1 mM mito-ACS in pure deionized water was freshly prepared. The measured solutions of probe with ClO^- were prepared by diluting 20 μL probe with PBS buffer solution (10 mM, pH 5), and then appropriate volume of ClO^- stock solution was added to ensure a final volume of 2 mL. The resulting solutions were shaken well and measured after 5 minutes. The same method was applied to the selectivity experiments. And the different pH solutions were adjusted by adding minimum volumes of NaOH (0.2 M) or HCl (0.2 M) with fresh PBS (10 mM, pH = 7.4). The fluorescence spectrums were collected with the excited wavelength of 480 nm and the slit widths of 2.0 nm.

2.4. Cell Viability Assay

HeLa cells were incubated in Dulbeccos modified Eagles medium (DMEM) supplement with 10% (v/v) Fetal Fovine Serum (FBS, Gibco), 100 U/mL penicillin, and 100 μg/mL streptomycin at 37 ^{o}C with 5 % CO2 in appropriate humidity. Before MTT test, HeLa cells (10^5 cells/well) were dispersed in a 96-well cell culture plate, and filled to 200 μL per well. 24 hours after incubation, the medium was removed and the cells were supplemented with medium containing mito-ACS of different concentrations (0, 5, 10, 15, 20 μM) and cultured for 24 hours. Cells incubated with no probe were used as blank control. After removal of the medium, 100 μL MTT solutions 5 mg/ mL) was added to each well away from light. After 4 hours, the MTT solutions were removed, and 200 μL of DMSO was added to each well to fully dissolve the formed formazan crystals by a shaker. Finally, a microplate reader was used to measure the absorbance at 490 nm.

2.5. Confocal Fluorescence Imaging

Confocal Fluorescence Imaging was collected on a Leica SP 8 confocal laser scanning microscope. To investigate the response ability of mito-ACS to ClO^- in *vivo*, Hela cells were divided into 4 groups. The control group of Hela cells were treated with probe mito-ACS (5 μM) for 30 minutes. and a parallel group of Hela cells were pretreated with N-acetylcysteine (NAC, 500 μM) for 2 h and then treated with NaClO (30 μM). To detect the exogenous ClO^-, the third group of Hela cells

 doi:10.20944/preprints202308.1195.v1

were treated with mito-ACS (5 μM) for 30 min, then treated with NaClO (30 μM) for another 30 minutes. To detect the endogenous ClO^-, the fourth group of Hela cells were treated with Lipopolysaccharide (LPS, 1 μg/mL) and phorbol 12-myristate 13-acetate (PMA, 1 μg/mL) for 12 h, then treated with probe mito-ACS (5 μM) for 30 minutes. The cells were washed by PBS (pH 7.4) for three times before imaging and fluorescence was collected in red channel (580–620 nm) with the excitation wavelength at 488 nm. To determine the subcellular localization, mito-ACS (5 μM) and mito-Tracker Green (200 nM) were co-incubated in cells for 30 min, then washed by PBS for three times. The fluorescence was collected in green channel (λex = 488 nm, λem = 500–520 nm) and red channel (λex = 488 nm, λem = 600–620 nm).

3. Results

The spectroscopic properties of probe **mito-ACS** and its response to ClO^- were first investigated in pure deionized water. The probe itself was nearly nonfluorescent (Φ = 0.06), and the absorbance peak was located at 492 nm (ε = 11250 M^{-1} cm^{-1}, **Figure 2a**). Upon the addition of ClO^- (3 equiv.), the absorbance of oxidation product displayed blue-shifted relative to **mito-ACS**: 479 nm versus 492 nm, and strong fluorescence emission at 575 nm appeared (Fig.S1). The fluorescence quantum yield was up to 0.28 in the presence of ClO^-. This large change in emission intensity minimizes the role of the initial probe with a large Stokes shift (96 nm) which allows clear separation of excitation and emission. According to the experimental results and previously reported work, probe **mito-ACS** exhibited weak fluorescence due to the electron donor ability of the thioether group. Upon the addition of ClO^-, the thiother group was oxidized to form a sulfoxide group, which suppressed the fluorescence quenching through a photo-induced electron transfer (PET) mechanism. To confirm this conjecture, we checked the mixture of **mito-ACS** and ClO^- by ESI-MS. As shown in Figure S2, the m/z peak of the oxidation product of **mito-ACS** was found, the main peak of 742.20, which is in agreement with the theoretical calculation values of [**mito-ACSO**]$^+$: 742.2176. This result supports the formation of the sensing product, sulfoxide from oxidation of the probes by ClO^-. Next, given the probe's initial design, we evaluated the pH influence on **mito-ACS**. As shown in Fig.S3, the probe exhibited an ignored fluorescence in a wide pH range of 3-10, indicating the thioether was insensitivity to the environmental pH change, while the strong fluorescence from the oxidation product remain stable in the pH of 3-9. Since the pH value of mitochondria is about 7.99, results indicate that **mito-ACS** could function properly in physiological conditions, including the mitochondria [39].

Then, titration experiments were carried to explore **mito-ACS**'s response to various equivalents of ClO^- upon excitation at 480 nm (100% aqueous media). The fluorescence intensity increased gradually with the concentration range of NaClO from 0 μM to 30 μM (**Figure 2b**). The fluorescence intensity of **mito-ACS** at 575 nm showed an excellent linear relationship (R^2=0.995) with ClO^- concentration (0–16 μM, **Figure 2c**), and the detection limit was calculated to be 23 nM (S/N=3), which makes the probe feasible for quantitatively detect mitochondrial ClO^- at trace levels [40]. Moreover, the reaction kinetics of **mito-ACS** (10 μM) with ClO^- (10 μM/20 μM) were also evaluated in pure aqueous media (pH = 7.4). As shown in **Figure 2d**, upon the addition of ClO^- to the probe solution, the fluorescence intensity at 575 nm enhanced rapidly and reached maximum within 6 s. Furthermore, the fluorescence signal of the oxidation product remains almost unchanged under continuous irradiation by a 450 W xenon lamp (**Figure S4**). Both the fast response time and high photostability are essential and suitable for the detection of ClO^- in vivo since the short-lived ClO^- and the complex biological environment.

Preprints (www.preprints.org) | NOT PEER-REVIEWED | Posted: 16 August 2023 doi:10.20944/preprints202308.1195.v1

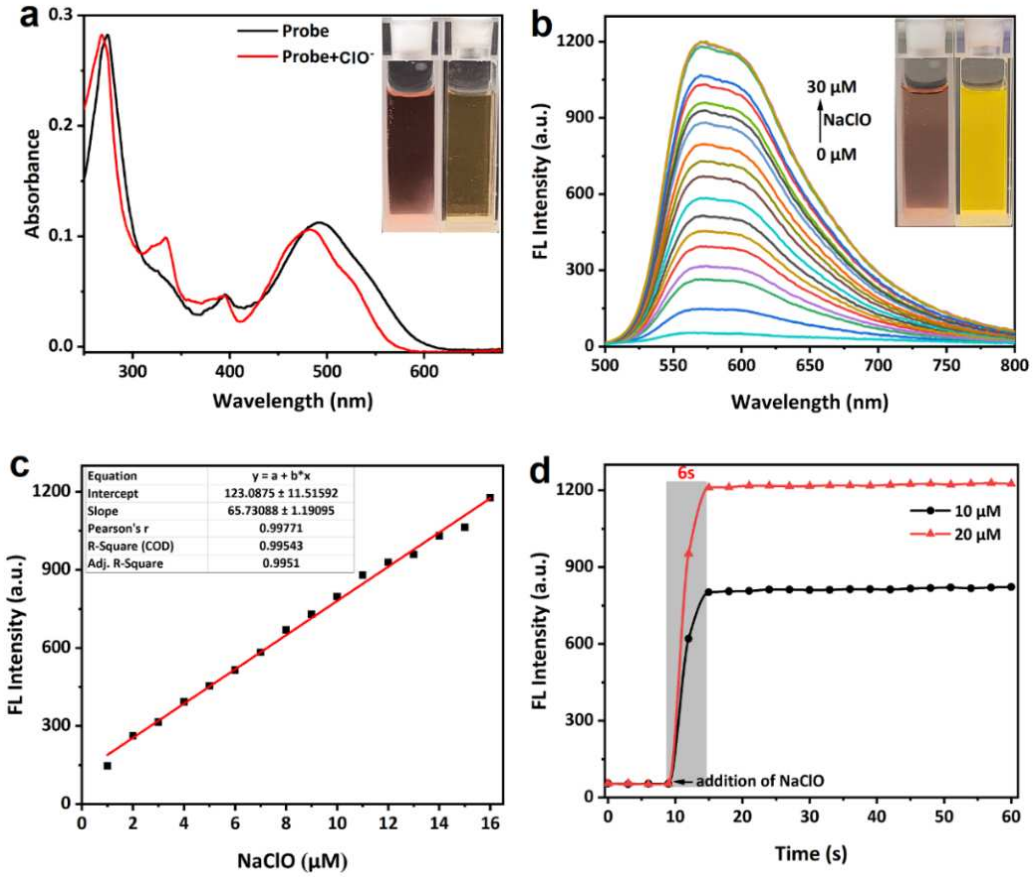

Figure 2. (**a**) UV–vis absorption (10 μM) and (**b**) fluorescence spectra (10 μM) changes of **mito-ACS** upon addition of increasing amount of NaOCl (0–30 μM), (**c**) fluorescence intensity at 575 nm of **mito-ACS** versus concentrations of ClO^-, (**d**) time-dependent fluorescence intensity changes of **mito-ACS** (10 μM) upon addition of ClO^- (10 μM/20 μM). (pure aqueous media, pH=7.4), λ_{exc} = 480 nm, slits = 2/2 nm. Inset: (a) the color and (b) fluorescence images of **mito-ACS** in the absence/presence of ClO^-.

The selectivity of the probe (10 μM) toward ClO^- and other bio-related interfering species including ROS/RNS (H_2O_2, •OH, O_2^{-}, $^1O_2$, ROO•, NO•, TBHP, •O^{t}Bu, metal ions (Ca^{2+}, Hg^{2+}, Mg^{2+}, Cu^{2+}, Cu^{+}, Zn^{2+}, Fe^{3+}, Fe^{2+}, Ag^{+} Al^{3+}), biothiols (Cys, Hcy, and GSH) was verified in the pure aqueous media [41]. As shown in **Figure 3a**, only ClO^- induced a strong fluorescence enhancement (>50 fold) while other species led to negligible response. Notably, hydroxyl radical (•OH, highly reactive oxygen radical) and Hg^{2+} (highly reactive with sulfur atom) did not noticeably enhance the fluorescence intensity of **mito-ACS**. In addition, the interference experiments were further studied by adding ClO^- (30 μM) to the probe in the presence of the competing species (100 μM), as shown in **Figure 3b**, **mito-ACS** displayed similar results in the fluorescence enhancement even in the presence of the interfering species. And lower fluorescence enhancements were observed in the presence of Fe^{2+} and biothios (Cys, Hcy, and GSH). This could attribute to their reducing properties reacting with ClO^-, thereby consuming ClO^- to some extent, leading to the fluorescence intensity decrease. Nevertheless, the ClO^- still triggered obvious fluorescence enhancement (> 20 folds) compared to the probe itself, respectively. The above results indicate that **mito-ACS** exhibits excellent selectivity to ClO^- in the presence of potential biological interferences, further confirming the potential of the probe to detect ClO^- in complex biological systems.

Preprints (www.preprints.org) | NOT PEER-REVIEWED | Posted: 16 August 2023 doi:10.20944/preprints202308.1195.v1

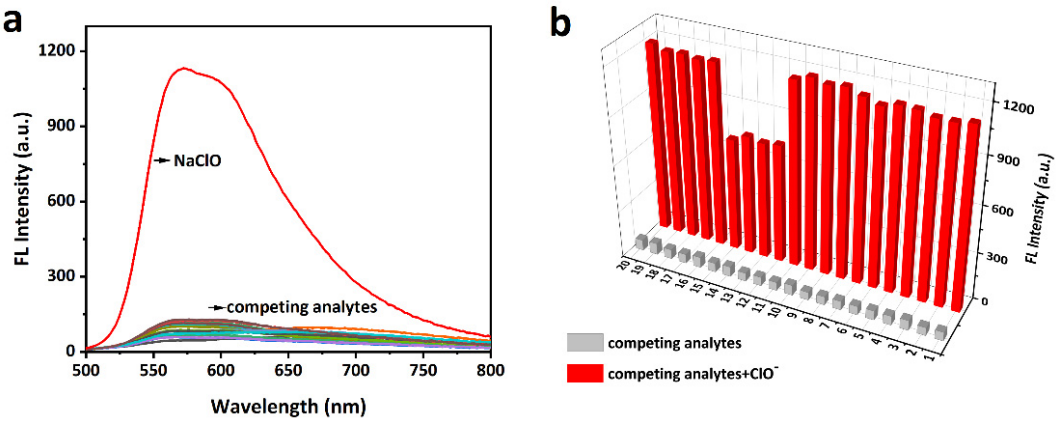

Figure 3. (**a**) Fluorescence emission spectra of **mito-ACS** (10 μM) with ClO^- (30 μM) and competing analytes (100 μM). (**b**) Fluorescence spectra response of **mito-ACS** (10 μM) with various analytes (100 μM) in response to ClO^- (30 μM). (1–20: H_2O_2, •OH, O_2^-, ROO•, NO•, TBHP, •OtBu, $ONOO^-$, Ca^{2+}, Mg^{2+}, Cu^{2+}, Fe^{2+}, Hcy, Cys, GSH, Hg^{2+}, Cu^+, Fe^{3+}, Zn^{2+}, Al^{3+}. (pure aqueous media, pH = 7.4), λ_{exc} = 480 nm, slits = 2/2 nm.

Based on the excellent response of **mito-ACS** to hypochlorous acid in *vitro*, we further explored the capability of probes for mitochondrial ClO^- imaging in living Hela cells. Before imaging, the standard MTT assay was conducted to evaluate the biocompatibility of **mito-ACS**. As shown in **Figure S5**, compared with the control group (cells without probe), the relative cell viability was up to 95% after incubated with 20 μM **mito-ACS** for 24 h, suggesting the probe possesses negligible cytotoxicity and good biocompatibility. In the next step, the mitochondria targeting ability was investigated with the colocalization experiment by co-incubating **mito-ACS** (5 μM) and the Mito-Tracker Green (200 nM, a commercial mitochondrial targeting dye). The green fluorescence from the Mito-Tracker Green and red fluorescence from **mito-ACS** treated with 30 μM ClO^- overlapped well (**Figure 4a–d**). Moreover, a high Pearson's coefficient of 0.952 has obtained from the intensity correlation plots (**Figure 4e**) and the fluorescence intensity profile of regions of interest (ROI) across HeLa cells in two channels also varied synchronously (**Figure 4f**). Colocalization experiments showed that **mito-ACS** possessed good cell membrane permeability and accurate mitochondria-targeting ability. These properties could be attributed to the introduction of triphenylphosphonium, a function group that aggregated the probe in mitochondria and also increased the probe's water solubility.

Finally, cell imaging experiments were carried out to evaluate the response ability of **moto-ACS** to ClO^- in living Hela cells. LPS and phorbol 12-myristate 13-acetate PMA are the known stimulants for cells to produce endogenous ClO^- while the NAC could remove the ROS including ClO^- [26,42].Four groups of experiments were set as the following: (1) incubation with probe (5 μM) for 30 minutes as control, (2) incubation with NAC (500 μM) for 2 h then probe (5 μM) for 30 minutes, (3) incubation with probe (5 μM) for 30 minutes then NaClO (30 μM), (4) incubation with LPS and PMA (1.0 mg mL^{-1}) for 2 h then probe (5 μM). As shown in Figure 4, the controlled Hela cells displayed a weak fluorescence (**Figure 5a–c**). Upon treatment with NAC, the fluorescence decreased significantly (**Figure 5d–f**), indicating that a small concentration of ClO^- exists in cells and the probe exhibited high sensitivity to the variation of ClO^- concentration. And as we expected, the fluorescence intensities were greatly enhanced under the LPS, PMA, and NaClO stimulation (**Figure 5g–i and Figure 5j–l**). Comparing the fluorescence intensities from the four groups (**Figure 5m**), we concluded that **mito-ACS** could be stained in mitochondria accurately and was well-suited for monitoring exogenous and endogenous ClO^- inside living Hela cells.

Preprints (www.preprints.org) | NOT PEER-REVIEWED | Posted: 16 August 2023 doi:10.20944/preprints202308.1195.v1

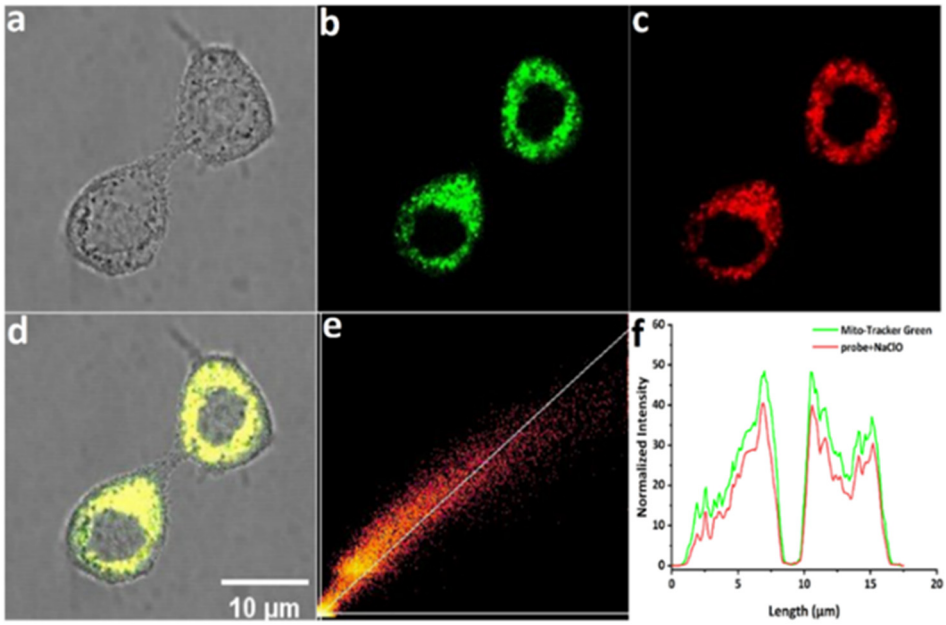

Figure 4. Confocal fluorescence images of living Hela cells incubated with **mito-ACS**(5 μM) and Mito-Tracker Green for 30 min: (**a**) bright-field imaging; (**b**) fluorescence imaging of Mito-Tracker Green (200 nM) in the green channel (λ_{exc} = 488 nm, λ_{em} = 500–520 nm); (**c**) fluorescence imaging of **mito-ACS** in the red channel (λ_{exc} = 488 nm, λ_{em} = 600–620 nm); (**d**) merged imaging of b and c; (**e**) intensity correlation of **mito-ACS** and Mito-Tracker Green (**f**) intensity distribution of the linear region of living Hela cells co-stained with **mito-ACS** and Mito-Tracker Green. Scale bar: 10 μm.

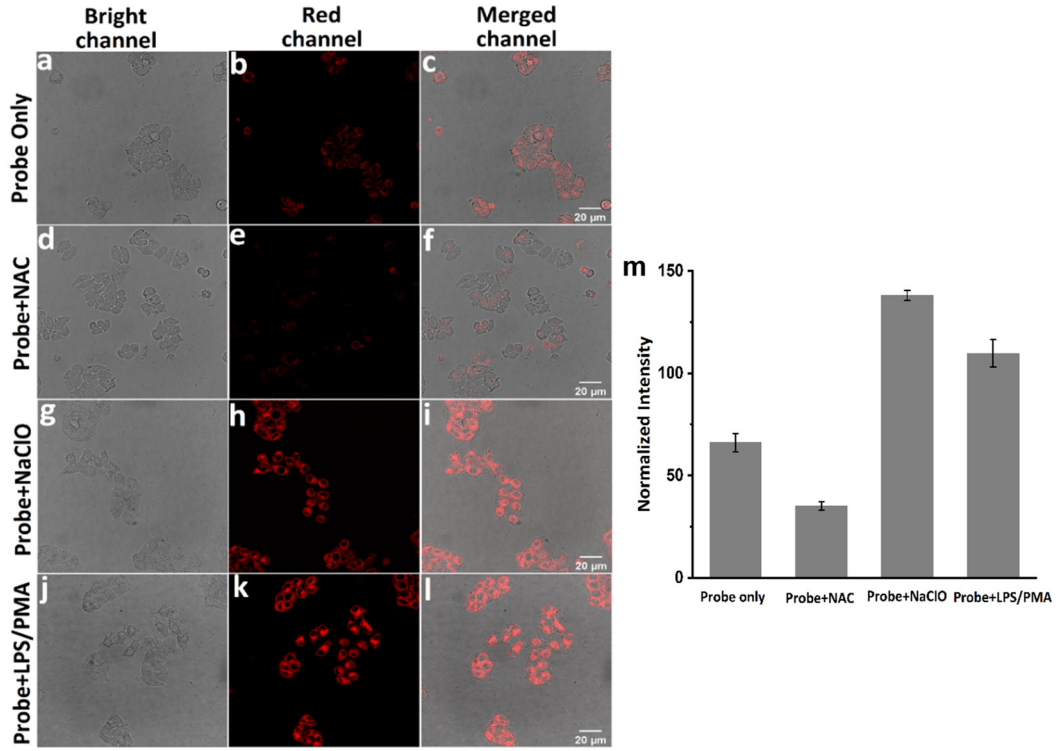

Figure 5. Confocal fluorescence images of living Hela cells incubated with (**a-c**) blank control, **mito-ACS** (5 μM) for 30 min; (**d-f**) NAC (500 μM) for 2h, then **mito-ACS** (5 μM) for 30 min, (**g-i**) **mito-ACS** (5 μM) for 30 min then NaClO (30 μM) for 30 min; (**j-l**) LPS and PMA (1.0 mg mL^{-1}) for 2h then **mito-ACS** (5 μM) for 30 min.respectively; (**m**) Normalized fluorescence intensity of cells in panels (**b**) to (**k**). λ_{exc} = 488 nm, λ_{em} =580- 620 nm, Scale bars are 20 μm.

4. Conclusions

In summary, we have presented the design strategy, synthesis, and practical application of a new probe, **mito-ACS**, for ClO^- detection in pure aqueous media and living Hela cells. **Mito-ACS** contains an anthracene carboxyimide core with red emission and a hypochlorite-triggered fluorescence "off−on" switch-thioether that affords excellent sensitivity. Surprisingly, the introduction of triphenylphosphonium makes the probe completely soluble in water and selectively localizes to mitochondria. Spectrometric analysis showed **mito-ACS** possess desirable optical properties in imaging ClO^-, such as high selectivity, fast response, and large Stokes shift. Furthermore, confocal fluorescence imaging revealed **mito-ACS** successfully achieved the monitoring of exogenous and endogenous mitochondrial ClO^- with low cytotoxicity. These features make **mito-ACS** uniquely suited for exploring ClO^- biology under a variety of physiological and pathological contexts.

Supplementary Materials: The following supporting information can be downloaded at the website of this paper posted on Preprints.org, Figure S1: Fluorescence spectra of the probe **mito-ACS** (10 μM) with and without excessive ClO^- (30 μM) in pure aqueous media; Figure. S2: MS-ESI spectra of **mito-ACS** and the reaction mixture of **mito-ACS** with NaOCl; Figure. S3: Time-dependent fluorescence intensity changes of **mito-ACS** (10 μM) under the irradiation by a 450w lamp; Figure. S4: Fluorescence response of **mito-ACS** (10 μM) in the absence and presence of NaOCl (30 μM) at different pH solutions; Figure. S5: Cell viability of HeLa cells treated with different concentrations of **mito-ACS** (0, 5, 10, 15, 20 μM) for 24 h; Figure. S6: ^{1}H NMR spectrum of **1** in $CDCl_3$; Figure. S7: ^{13}C NMR spectrum of **1** in $CDCl_3$; Figure. S8: ^{1}H NMR spectrum of **2** in $CDCl_3$; Figure. S9: ^{13}C NMR spectrum of **2** in $CDCl_3$; Figure. S10: ^{1}H NMR spectrum of **3** in $CDCl_3$; Figure. S11: ^{13}C NMR spectrum of **3** in $CDCl_3$; Figure. S12: ^{1}H NMR spectrum of **mito-ACS** in $CDCl_3$; Figure. S13: ^{13}C NMR spectrum of **mito-ACS** in $CDCl_3$.

Author Contributions: X.L.; Conceptualization, Methodology, Writing—original draft, Data curation. G.Z.; Investigation. Y.W. and W.Z.; Conceptualization, Formal analysis, Data curation, Writing—review and editing, Supervision, Project administration, Funding acquisition. All authors have read and agreed to the published version of the manuscript.

Funding: This work was supported by the Natural Science Foundation of China (grant 21672160), and Science and Technology Plan Projects of Tangshan City (22130218H).

Institutional Review Board Statement: Not applicable.

Informed Consent Statement: Not applicable.

Data Availability Statement: Not applicable.

Acknowledgments: The authors thank Prof. Nathaniel Finney with the experiments and valuable discussion.

Conflicts of Interest: The authors declare no conflict of interest.

References

1. Hawkins, C. L.; Davies, M. J., Role of myeloperoxidase and oxidant formation in the extracellular environment in inflammation-induced tissue damage. *Free Radical Biol. Med.* **2021,** 172, 633-651.
2. Zhang, R.; Song, B.; Yuan, J., Bioanalytical methods for hypochlorous acid detection: Recent advances and challenges. *TrAC, Trends Anal. Chem.* **2018,** 99, 1-33.
3. Brandes, R. P.; Rezende, F.; Schröder, K., Redox Regulation Beyond ROS. *Circ. Res.* **2018,** 123, (3), 326-328.
4. Clayton, G. E.; Thorn, R. M. S.; Reynolds, D. M., The efficacy of chlorine-based disinfectants against planktonic and biofilm bacteria for decentralised point-of-use drinking water. *npj Clean Water* **2021,** 4, (1), 48.
5. de Araujo, T. H.; Okada, S. S.; Ghosn, E. E.; Taniwaki, N. N.; Rodrigues, M. R.; de Almeida, S. R.; Mortara, R. A.; Russo, M.; Campa, A.; Albuquerque, R. C., Intracellular localization of myeloperoxidase in murine peritoneal B-lymphocytes and macrophages. *Cell. Immunol.* **2013,** 281, (1), 27-30.
6. Aratani, Y., Myeloperoxidase: Its role for host defense, inflammation, and neutrophil function. *Arch. Biochem. Biophys.* **2018,** 640, 47-52.
7. Casciaro, M.; Di Salvo, E.; Pace, E.; Ventura-Spagnolo, E.; Navarra, M.; Gangemi, S., Chlorinative stress in age-related diseases: a literature review. *Immun. Ageing* **2017,** 14, (1), 21.
8. Wei, P.; Liu, L.; Yuan, W.; Yang, J.; Li, R.; Yi, T., A fluorescent probe operating under weak acidic conditions for the visualization of HOCl in solid tumors in vivo. *Sci. China: Chem* **2020,** 63, (8), 1153-1158.

9. Zhan, Z.; Lei, Q.; Dai, Y.; Wang, D.; Yu, Q.; Lv, Y.; Li, W., Simultaneous Monitoring of HOCl and Viscosity with Drug-Induced Pyroptosis in Live Cells and Acute Lung Injury. *Anal. Chem.* **2022,** 94, (35), 12144-12151.
10. Feng, H.; Zhang, Z.; Meng, Q.; Jia, H.; Wang, Y.; Zhang, R., Rapid Response Fluorescence Probe Enabled In Vivo Diagnosis and Assessing Treatment Response of Hypochlorous Acid-Mediated Rheumatoid Arthritis. *Adv. Sci.* **2018,** 5, (8), 1800397.
11. Andersen, J. K., Oxidative stress in neurodegeneration: cause or consequence? *Nat. Med.* **2004,** 10, (7), 18-25.
12. Sabharwal, S. S.; Schumacker, P. T., Mitochondrial ROS in cancer: initiators, amplifiers or an Achilles' heel? *Nat. Rev. Cancer* **2014,** 14, (11), 709-721.
13. Hoye, A. T.; Davoren, J. E.; Wipf, P.; Fink, M. P.; Kagan, V. E., Targeting Mitochondria. *Acc. Chem. Res.* **2008,** 41, (1), 87-97.
14. Yang, Y.-t. T.; Whiteman, M.; Gieseg, S. P., HOCl causes necrotic cell death in human monocyte derived macrophages through calcium dependent calpain activation. *Biochim. Biophys. Acta, Mol. Cell Res.* **2012,** 1823, (2), 420-429.
15. Zhou, J.; Li, L.; Shi, W.; Gao, X.; Li, X.; Ma, H., HOCl can appear in the mitochondria of macrophages during bacterial infection as revealed by a sensitive mitochondrial-targeting fluorescent probe. *Chem. Sci.* **2015,** 6, (8), 4884-4888.
16. Geng, Y.; Wang, Z.; Zhou, J.; Zhu, M.; Liu, J.; James, T. D., Recent progress in the development of fluorescent probes for imaging pathological oxidative stress. *Chem. Soc. Rev.* **2023,** 52, (11), 3873-3926.
17. Nguyen, V.-N.; Ha, J.; Cho, M.; Li, H.; Swamy, K. M. K.; Yoon, J., Recent developments of BODIPY-based colorimetric and fluorescent probes for the detection of reactive oxygen/nitrogen species and cancer diagnosis. *Coord. Chem. Rev.* **2021,** 439, 213936.
18. Yan, F.; Zang, Y.; Sun, J.; Sun, Z.; Zhang, H., Sensing mechanism of reactive oxygen species optical detection. *TrAC, Trends Anal. Chem.* **2020,** 131, 116009.
19. Song, X.; Li, C.; Wang, Y.; Wang, D.; Liu, Z., A ratiometric two-photon fluorescence probe for monitoring mitochondrial HOCl produced during the traumatic brain injury process. *Sens. Actuators, B* **2020,** 311, 127895.
20. Shen, S.-L.; Huang, X.-Q.; Zhang, Y.-Y.; Zhu, Y.; Hou, C.; Ge, Y.-Q.; Cao, X.-Q., Ratiometric fluorescent probe for the detection of HOCl in lysosomes based on FRET strategy. *Sens. Actuators, B* **2018,** 263, 252-257.
21. Gao, P.; Pan, W.; Li, N.; Tang, B., Fluorescent probes for organelle-targeted bioactive species imaging. *Chem. Sci.* **2019,** 10, (24), 6035-6071.
22. Ji-Ting, H.; Nahyun, K.; Shan, W.; Bingya, W.; Xiaojun, H.; Juyoung, Y.; Jianliang, S., Sulfur-based fluorescent probes for HOCl: Mechanisms, design, and applications. *Coord. Chem. Rev.* **2021**, 214232.
23. Nahyun, K.; Yahui, C.; Xiaoqiang, C.; Myung Hwa, K.; Juyoung, Y., Recent progress on small molecule-based fluorescent imaging probes for hypochlorous acid (HOCl)/hypochlorite (OCl^-). *Dyes Pigm.* **2022**, 200, 110132.
24. Ren, M.; Zhou, K.; He, L.; Lin, W., Mitochondria and lysosome-targetable fluorescent probes for HOCl: recent advances and perspectives. *J. Mater. Chem. B* **2018**, 6,1716-1733.
25. Ma, C.; Zhong, G.; Zhao, Y.; Zhang, P.; Fu, Y.; Shen, B., Recent development of synthetic probes for detection of hypochlorous acid/hypochlorite. *Spectrochim. Acta, Part A* **2020**, 240, 118545.
26. Yuan, L.; Wang, L.; Agrawalla, B. K.; Park, S.-J.; Zhu, H.; Sivaraman, B.; Peng, J.; Xu, Q.-H.; Chang, Y.-T., Development of Targetable Two-Photon Fluorescent Probes to Image Hypochlorous Acid in Mitochondria and Lysosome in Live Cell and Inflamed Mouse Model. *J. Am. Chem. Soc.* **2015,** 137, (18), 5930-5938.
27. Winterbourn, C. C., Biological reactivity and biomarkers of the neutrophil oxidant, hypochlorous acid. *Toxicology* **2002,** 181-182, 223-227.
28. Aratani, Y.; Koyama, H.; Nyui, S.-i.; Suzuki, K.; Kura, F.; Maeda, N., Severe Impairment in Early Host Defense againstCandida albicans in Mice Deficient in Myeloperoxidase. *Infect. Immun.* **1999,** 67, (4), 1828-1836.
29. Marx, V., Probes: paths to photostability. *Nat. Methods* **2015,** 12, (3), 187-190.
30. Dai, J.; Wu, Z.; Li, D.; Peng, G.; Liu, G.; Zhou, R.; Wang, C.; Yan, X.; Liu, F.; Sun, P.; Zhou, J.; Lu, G., Super-resolution dynamic tracking of cellular lipid droplets employing with a photostable deep red fluorogenic probe. *Biosens. Bioelectron.* **2023,** 229, 115243.
31. Hu, Q.; Duan, C.; Wu, J.; Su, D.; Zeng, L.; Sheng, R., Colorimetric and Ratiometric Chemosensor for Visual Detection of Gaseous Phosgene Based on Anthracene Carboxyimide Membrane. *Anal. Chem.* **2018,** 90, (14), 8686-8691.
32. Xu, J.; Niu, G.; Wei, X.; Lan, M.; Zeng, L.; Kinsella, J. M.; Sheng, R., A family of multi-color anthracene carboxyimides: Synthesis, spectroscopic properties, solvatochromic fluorescence and bio-imaging application. *Dyes Pigm.* **2017,** 139, 166-173.
33. Zeng, L.; Zeng, H.; Wang, S.; Wang, S.; Hou, J.-T.; Yoon, J., A paper-based chemosensor for highly specific, ultrasensitive, and instantaneous visual detection of toxic phosgene. *Chem. Commun.* **2019,** 55, (91), 13753-13756.

34. Hou, J.-T.; Kwon, N.; Wang, S.; Wang, B.; He, X.; Yoon, J.; Shen, J., Sulfur-based fluorescent probes for HOCl: Mechanisms, design, and applications. *Coord. Chem. Rev.* **2022,** 450, 214232.
35. Zhou, G.; Hou, S.; Zhao, N.; Finney, N.; Wang, Y., A novel colorimetric and ratiometric fluorescent probe for monitoring lysosomal HOCl in real time. *Dyes Pigm.* **2022,** 204, 110394.
36. de Silva, A. P., Crossing the divide: Experiences of taking fluorescent PET (photoinduced electron transfer) sensing/switching systems from solution to solid. *Dyes Pigm.* **2022,** 204, 110453.
37. Yao, J. H.; Chi, C.; Wu, J.; Loh, K.-P., Bisanthracene Bis(dicarboxylic imide)s as Soluble and Stable NIR Dyes. *Chem. - Eur. J.***2009,** 15, (37), 9299-9302.
38. Yamaguchi, Y.; Ochi, T.; Wakamiya, T.; Matsubara, Y.; Yoshida, Z.-i., New Fluorophores with Rod-Shaped Polycyano π-Conjugated Structures: Synthesis and Photophysical Properties. *Org. Lett.* **2006,** 8, (4), 717-720.
39. KETTLE, A. J.; GEDYE, C. A.; WINTERBOURN, C. C., Mechanism of inactivation of myeloperoxidase by 4-aminobenzoic acid hydrazide. *Biochem. J* **1997,** 321, (2), 503-508.
40. Zhu, B.; Gao, C.; Zhao, Y.; Liu, C.; Li, Y.; Wei, Q.; Ma, Z.; Du, B.; Zhang, X., A 4-hydroxynaphthalimide-derived ratiometric fluorescent chemodosimeter for imaging palladium in living cells. *Chem. Commun.* **2011,** 47, (30), 8656-8658.
41. Zeng, L.; Xia, T.; Hu, W.; Chen, S.; Chi, S.; Lei, Y.; Liu, Z., Visualizing the Regulation of Hydroxyl Radical Level by Superoxide Dismutase via a Specific Molecular Probe. *Anal Chem* **2018,** 90, (2), 1317-1324.
42. Bodega, G.; Alique, M.; Puebla, L.; Carracedo, J.; Ramírez, R. M., Microvesicles: ROS scavengers and ROS producers. *J. Extracell. Vesicles* **2019,** 8, (1), 1626654.